Dinocyst records from deep cores reveal a reversed salinity gradient in the Caspian Sea at 8.5–4.0 cal ka BP

Suzanne A.G. Leroy, Lourdes López-Merino, Nina Kozina

Dinocyst records from deep cores reveal a reversed salinity gradient in the Caspian Sea at 8.5 – 4.0 cal. ka BP

Suzanne A. G. Leroy[1], Lourdes López-Merino[2] and Nina Kozina[3]

1 Aix Marseille Univ, CNRS, Minist Culture, LAMPEA, UMR 7269, 5 rue du Château de l'Horloge, 13094, Aix-en-Provence, France, leroy@mmsh.univ-aix.fr, corresponding author
2 Department of Geography, Geology and the Environment, Kingston University, Penrhyn Road, Kingston upon Thames, Surrey KT1 2EE, UK, l.lopez-merino@kingston.ac.uk; lolome@hotmail.es
3 Shirshov Institute of Oceanology, Russian Academy of Science, Russia. kozina_nina@bk.ru

Abstract

Understanding the long-term environmental forcings driving Caspian Sea (CS) water levels is of utmost importance, not only owing to its large size, or to the surrounding developing economies but also to improve global climate models and forecasts. However, Late Quaternary CS level changes and their amplitude are mostly documented from incomplete coastal sediment records. Because of the CS idiosyncrasies, that behaves neither as a sea nor as a lake, the methods used to reconstruct water levels in the global ocean or in freshwater lakes do not always apply.

Here, we propose a first step toward the use of dinoflagellate cysts records to reconstruct qualitative changes in water mass, focusing on new and published deep-water sedimentary sequences from the south and middle CS basins. Trends in water level changes are reconstructed on the relative proportions of dinocyst assemblages with different levels of brackishness.

A higher highstand than previously seen is reconstructed post-Mangyshlak lowstand. A reverse water flow gradient from S to N, not previously detected, is identified at 8.5-8 to 4 cal. ka BP. A major turnover in dinocyst assemblage is found at 4 cal. ka BP. While the Volga River is the main source of water nowadays, we propose that the source of water to maintain the 8.5-8 to 4 cal. ka BP highstand is the now-disconnected drainage basin of the Amu-Darya. The CS was at that time most likely strongly influenced by low latitude climates, with more precipitation over the Karakum and, perhaps, even indirect monsoonal influence.

Keywords: Quaternary; Palaeolimnology; Southwestern Asia; Pontocaspian; micropalaeontology dinocyst; water flow direction; Amu-Darya

1. Introduction

The long-term water-level histories of ancient lakes are fingerprinted in their sediments, and both biological and non-biological proxies may be used to unravel long-term environmental changes. In fact, numerous examples of long-term rapid water-level changes with large vertical amplitudes (>500 m)

have been exposed for large lakes, such as Tanganyika, Victoria, Malawi (Cohen et al. 2007), Baikal (Colman et al. 1993), and Issyk-Kul (Gebhardt et al. 2017). The annual to decadal amplitudes observed with the instrumental record are in the order of 10 to 50 times smaller than the centennial to millennial ones (Lahijani et al. 2016), as they only capture the short-term variability. In addition, the instrumental record of large lakes dates back to the 19th century at most (Leroy et al. in press). Of interest in large lakes is the understanding of long-term water level fluctuations, as they may be linked to climate and, thus, used to forecast future water-level changes that will affect humans. In addition, large lakes, especially endorheic ones, are very susceptible to climatic change (Arpe et al. 2018), and, owing to their size, they are also vulnerable to hydrographic changes that may affect dramatically exchanges between water masses (Lahijani et al. in press).

The Caspian Sea (CS) is the largest inland lake in the world, with a water area of 386,400 km^2 and volume of 78,200 km^3, three times larger than Lake Baikal. The detailed history of CS Late Quaternary water level changes is notoriously poorly known, even for the last millennia (Naderi Beni et al. 2013; Bezrodnykh and Sorokin 2016; Leroy et al. in press). The fragmentary known information indicates that CS level changes, at times rapid, have affected large basin areas, especially the shallow north basin and the now exposed low-lying Caspian depression (Fig. 1). Continuous deep-water sedimentary sequences are the appropriated geo-environmental archives to unravel information on water level changes, ideally when taken below the lowest lowstand and away from delta influence prone to varying sedimentation rates

and mass-wasting movements.

Fig. 1 Leroy et al.

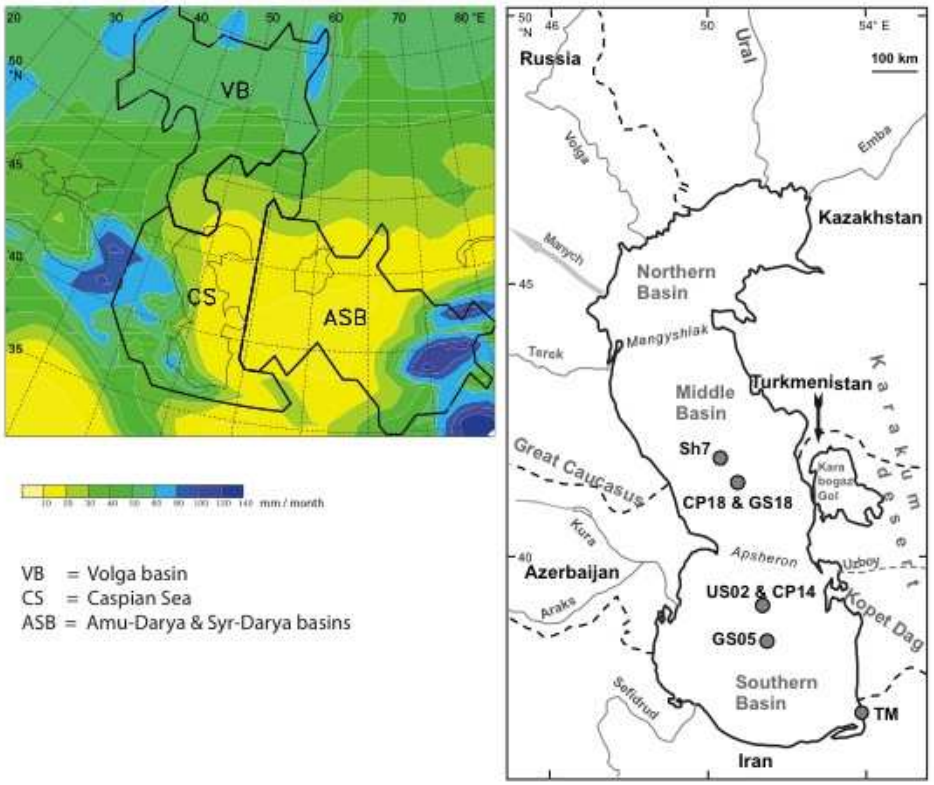

***Figure 1**: The Caspian Sea setting. A: Precipitation (mm/month) and main drainage basins influencing the Caspian Sea (CS = Caspian Sea, ASB = Aral Sea Basin); B: Location of the Caspian Sea and of the sites mentioned in the text. The grey arrow follows the Manych spillway. The black arrow shows where Turkmenistan is.*

However, classical methods to reconstruct sea-level change in global ocean settings, such as foraminifera, often do not work well in the CS due to its unique features (e.g. absence of foraminifera below 50 m water depth, Boomer et al. 2005; Yanko-Hombach 2007; Kh. Saidova pers. comm. 2011). The same happens with other methods used to reconstruct water levels in freshwater lakes, such as diatoms (Svalnov and Kazarina 2008; Leroy et al. 2018). Therefore, geoscientists working on the CS must find additional proxies. In this paper, we evaluate the palaeoenvironmental potential of organic-walled dinoflagellates, unicellular phytoplankton organisms that form cysts that may be preserved in sediments and are called dinocysts. A recent major compilation of surface samples in the Pontocaspian region has shown

that dinocyst assemblages are sensitive to salinity changes, amongst other parameters, and may provide invaluable qualitative information to detect the flow of water masses, as well as water-level fluctuations at millennial, centennial and, even, decadal scales (Mudie et al. 2017).

This work aims to test the use of dinocyst records to reconstruct changes in CS water masses and levels. The available continuous sequences with detailed dinocyst records (i.e. dinocyst counts at least >100 per sample) covering the Late Quaternary derive from deep-water sequences (> 315 m) located at the middle and south CS basins only (Leroy et al. 2007, 2013c, 2014). A lagoon sequence, core TM (Leroy et al. 2013a), from the SE coastal basin covers the Late Quaternary chronology and has appropriate dinocyst counts. However, its lagoonal character is reflected in a large hiatus. In addition, several Holocene palynological records from cores from the north basin are also available (Richards et al. 2014). However they do not cover the Pleistocene-Holocene transition, their dinocyst counts are low, and the presence of reworking material and erosional influence are noticeable as they are located in a deltaic environment. The specific objectives are three. First, to present the available Late Quaternary dinocyst records from the south and middle CS basins together with a new dinocyst record from the middle basin. Second, to compare the dinocyst records to previous water level reconstructions performed using other proxies and discuss dissimilarities. Third, to unravel water flow directions between the middle and the south basins in order to detect any major change in palaeo-river discharge.

2 Setting

2.1 Caspian Sea setting and previous reconstructions

The CS provides many economic resources to the area, such as the rich oil and gas fields as well as fisheries, including sturgeon for caviar. The CS is a large endorheic lake made up of three basins, deepening from the very shallow north (5 m), via the deep middle (maximal water depth of 788 m), to the deepest south basin (maximal water depth 1025 m) (Kostianoy and Kosarev 2005). CS water level, as measured in 2018, is at 28 m bsl (Leroy et al. in press). The modern water surface salinity shows a gradient from freshwater in the north basin large Volga delta to 13 psu in the middle and south basins due to larger freshwater inflow in the north and larger evaporation in the south (Cazenave et al. 1997; Kostianoy and Kosarev 2005; Leroy et al. 2018, in press; Lahijani et al. in press).

The CS is fed by several rivers but receives none from the desertic east side. The main river contributing water to the CS is the Volga, representing 80-90% of the water inflow (Leroy et al. in press). The Volga has a catchment extending far north, reaching >60 °N in several places (Fig. 1). The CS level is affected by precipitation on the Volga catchment, especially by changes in summer precipitation and by evaporation over its surface, as well as by river inflow volume (Arpe et al. 2007, 2012). The catchment of the CS is under the influence of the Westerlies (Arpe et al. 2018). So far, available climatic models do not consider a dynamic CS surface in their simulations despite the effect that changes in the size of the largest inland water body in the world could have on climate. In fact, it has recently been shown that the CS size has a

clear influence on regional and, even to some instance, global climate (Arpe et al. 2018).

The main sources of information on CS levels are Varushchenko et al. (1987), Klige (1990), Rychagov (1997), Mamedov (1997), Chepalyga (2007), Svitoch (2009, 2012), and Kakroodi et al. (2012). Leroy et al. (in press) compiled the various CS level reconstructions, the comparison highlighting some similarities but, in general, a lack of spatiotemporal congruence between studies. In brief, these reconstructions indicate that the CS levels have changed by more than 150 m since the Last Glacial Maximum (LGM). During the deglaciation, the CS levels were rather high with a peak in the early Khvalynian at 50 m asl (although a revision might indicate only + 35 m, Makshaev et al. 2015; Arslanov et al. 2016). A rather short lowstand is reconstructed after the early Khvalynian highstand. This lowstand is followed by the late Khvalynian highstand whose upper boundary is classically located at the end of the Pleistocene. It seems that the CS experienced a major lowstand at the beginning of the Holocene, i.e. the Mangyshlak lowstand, with levels perhaps as low as 113 m bsl. The duration of this lowstand varies between 1 and 3 ka, and the CS levels rose thereafter, although with levels lower than during the Khvalynian. This period is known as the Neocaspian, that itself counts several, rather brief lowstands. Some authors make the Neocaspian start much later than 1-3 millennia after the Holocene onset according to mollusc assemblages, i.e. c. 7.4 cal. ka BP (published as c. 6.5 ^{14}C ka BP).

2.2 Idiosyncrasy of the CSL reconstruction

A small range of proxies has been used with varied success to produce the available CS level reconstructions. Lithology is the most common one, focusing on the occurrence of discontinuities, lateral facies change, channels, grain-size and carbonate content (Bezrodnykh and Sorokin 2016). Unfortunately, no comprehensive seismic studies of the CS are available. Two main reasons explain the paucity of seismic studies in such an economically and environmentally important area of the world. Firstly, because just few scientific studies have been undertaken so far, probably linked to the lack of research vessels and the large size of the area. Secondly, among the scarce work done on the Caspian basin, most of it has been performed by the petroleum industry, thus remaining confidential.

The most common biotic proxy applied so far in the CS is mollusc shells, used to reconstruct past salinities and/or depths mostly based on occurrences and, more rarely, assemblages (Svitoch 2009, 2012; Leroy et al. 2018). Moreover, mollusc shells are also used for Quaternary stratigraphy and as material for radiocarbon dating (Yanina 2013). The measurement of oxygen isotopes has been used in the CS on a lagoon (Kakroodi et al. 2015), on deep cores (Chalié et al. 1997; Ferronsky et al. 1999), as well as tested on various biota in a surface sediment transect (Leroy et al. 2018). The latter obtained mixed success, as more than one factor seem to drive oxygen isotope ratios, the best outcome of the $\delta^{18}O$ tests being with ostracods.

Other CS biotas include benthic ostracods (Boomer et al. 2005; Leroy et al. 2018) and diatoms, whose ecology is often poorly known. For the latter, many species are very euryhaline, thus not very informative, and problems of

preservation do occur (Leroy et al. 2018; Chalié pers. comm.). Benthic foraminifers live only down to 50 m water depth in the CS, drastically limiting their use (Boomer et al. 2005; Leroy et al. 2013b, 2018). Although molluscs and benthic ostracods are present down to the CS bottom, they dwell in low concentrations only (Leroy et al. 2018). Dinocysts are one of the rare aquatic biota remaining present at all depths in significant concentrations and in excellent preservation state. In brief, at depths deeper than the lowest water levels of the CS since the LGM, many biotic proxies are of limited use and remain in urgent need of calibration (Leroy et al. 2018).

3 Material and methods

3.1 The datasets

This work uses dinocyst records from three datasets (Table 1) from cores located in the deep south and middle CS basins (>315 m depth; Fig. 1). The dataset from the south basin is made of three complementary cores: a Kullenberg core GS05, a pilot core CP14 and an Usnel core US02 (Leroy et al. 2007, 2013c). The first dataset from the middle basin is made of two complementary cores: a Kullenberg core GS18 (called GS20 in Chalié et al. 1997; Ferronsky et al. 1999; Kuprin et al. 2003; Boomer et al. 2005; Tudryn et al. 2013, 2016) and a pilot core CP18 (Leroy et al. 2007, 2014). Each of these dinocyst datasets has already been discussed separately along with pollen data and dating information (Leroy et al. 2007, 2013c, 2014).

***Table 1**: Sediment cores from the middle and south basins of the CS discussed in this work.*

Data set	Core name	Latitude N, Longitude E	Water depth in m	Chronology	Reference
	Middle basin				
1	**Sh7**	41°49'14.10" 50°23'52.62"	749	tie points after comparison of palynological records with GS18 and GS05 (Table SI3)	This work
2	**CP18**	41°32'53" 51°06'04"	480	younger than GS18 with 35-95 cm overlap, established by comparison of palynological diagrams with core GS18	Leroy et al. (2007)
2	**GS18**	41°32'53" 51°06'04"	479	6 ^{14}C on ostracods; age-depth model after applying a 370-year reservoir effect, calibrating with the IntCal13.14C curve, and using a smooth spline solution (smooth factor of 0.3)	Leroy et al. (2014), Tudryn et al. (2016), this work

	South basin				
3	**US02**	39°16’ 51°28’	315	Radionuclides	Leroy et al. (2013b)
3	**CP14**	39°16’18” 51°27’47”	330	3 ^{14}C on bulk after correction for detritics: age-depth model after calibrating with IntCal98.14C curve, and and using linear interpolation between dates	Leroy et al. (2007)
3	**GS05**	38°45’39” 51°32’16”	518	18 ^{14}C on bulk carbonates and ostracods; age-depth model after applying a 370-year reservoir effect, calibrating with the IntCal09.14C curve, and using a smooth spline solution (smooth factor of 0.3)	Leroy et al. (2013c)

Twenty-two new dinocyst samples have been added at the base of core GS18 using the same age-depth model, cyst extraction and zonation methods as in the upper part of the core (Leroy et al. 2014) (SI 1). The lithology of this new interval is similar to the lithology of the upper part of the core, consisting of fine-grained sediments with bedding and in the lower part carbonate contents around 10% (Leroy et al., 2014). These basal samples were initially considered deposited under different taphonomy based on the mainly reworked pollen content. The reworked content was identified because of the corroded and darker aspect of the pollen grains. Dinocysts did not show signs of reworking. However, more recently Tudryn et al. (2016) indicated that the reworking was essentially from a strong Volga inflow. The pollen can be water transported hundreds of km along the Volga from its terrestrial source to the CS basin. However, the picture is very different with the dinocysts, as they could only come from a few tens of km from the north basin, since no dinoflagellates live in the Volga River. Therefore, the dinocysts are expected to be largely *in-situ*.

Together with the twenty-two new samples of core GS18, we present the palynological results of a new sequence from the middle basin, core Sh7, located ~65 km further north than core GS18 (Table 1, Fig. 1). This 600 cm long core of 14 cm diameter was taken in 2010 as part of a research programme of Lisitzyn (P.P. Shirshov Institute of Oceanology, Moscow). The palynological extraction, counting and zonation methods of the 31 samples analysed are the same as for the two other datasets (Leroy et al. 2007, 2013c, 2014). Six radiocarbon dates obtained from ostracods have yielded results that are not in stratigraphic order for an unknown reason (SI 2). Amongst the various reasons that could have affected the radiocarbon results other than just transport (reworking), are methane seepage and mud volcanoes (Leroy et al., 2018). Therefore, as the radiocarbon dates could not be used to build an age-depth model for core Sh7, the pollen and dinocyst records of core Sh7 have been compared with those from the nearby core GS18, with some

additional information from core GS05, in order to identify tie points that could shed light onto core Sh7 chronological framework. Sixteen tie points have been found combining common major changes, disappearances and appearances in pollen (twelve tie points) and dinocysts (four tie points) assemblages (Fig. 2, Table SI 3).

In all these datasets, a minimum of 100 dinocysts was counted and identified in most samples (except in some of the additional samples at the base of GS18). Varia includes unknown, reworked and undeterminable cysts. The total concentration of dinocysts is shown in dinocysts per ml of wet sediment. P/D is the ratio between pollen concentration and dinocyst concentration.

The granulometry on 39 samples of core Sh7 was obtained by sieving without HCl attack and the facies described according to the classification adopted at the Institute of Oceanology of Russian Academy of Sciences (Petelin 1967).

3.2 The taxa and their ecological requirements

The CS is clearly less diverse in dinoflagellate species than the Black Sea (Mudie et al. 2017). Moreover, fewer cysts are known than motile forms (Lewis et al. 2018). In what follows we summarise the requirements of the dinocysts found in the CS.

Pyxidinopsis psilata and *Spiniferites cruciformis* are often considered as living in salinities ≤7 psu (Dale 1996). However, they have been found at higher salinities up to 18 psu in some sites, but the cysts are present in low percentages only (Mudie et al. 2017). *Spiniferites belerius* seems to occur more frequently in waters with fluctuating salinities (Mudie et al. 2017).

The salinities in which *Impagidinium caspienense* lives are poorly known, as it is a new species apparently endemic to the CS, Aral Sea and Karabogaz-Gol with rare occurrences in the Black Sea (Mudie et al. 2017). Marret et al. (2004) have shown that it is very abundant in surface sediment samples of the CS with surface water salinities of 13 psu. As *I. caspienense* has been observed in the highly saline waters of the Karabogaz-Gol (Leroy et al. 2006), higher salinities are possible for this species. A link between the cyst *I. caspienense* and the motile stage *Gonyaulax baltica* has recently been established (Mudie et al. 2017; Mertens et al. 2017), with experimentation on cyst formation showing a lower limit at around 10-13 psu (Ellegaard et al. 2002). Hence, its salinity preference is taken as being close to 10 - >13 psu.

Lingulodinium machaerophorum is a rather ubiquitous species (Mertens et al. 2009; Leroy et al. 2013b; Mudie et al. 2017). The other taxa found in the palynological studies (i.e. *Caspidinium rugosum*, *C. rugosum rugosum* and *Pentapharsodinium dalei* cyst) are mostly present in low abundances, and their salinity ranges are not very well defined but seem broad (Mudie et al. 2017). Concerning nutrients, only *Brigantedinium* is heterotroph; the other species are autotroph, with *L. machaerophorum* being mixotroph (Mudie et al. 2017).

The statistical analysis of the oceanographic parameters of dinocysts in 181 modern samples in the Pontocaspian area (Mudie et al. 2017) shows that sea surface salinity, especially from January to March, is the main factor explaining dinocysts distribution. The second main factor is the sea surface

temperature, especially from January to March when ice forms. A limitation of this modern dataset is the scarcity of sites with salinities <8 psu, with the total absence of salinities <6 psu. The Khvalynian highstand assemblages dominated by *S. cruciformis* and *P. psilata*, not only in the CS (Leroy et al. 2013c, 2014) but also in its equivalent in the Black Sea (Shumilovskikh et al. 2014), do not have modern analogues so far.

Briefly, going any further with attributing fixed ranges of salinities to dinocysts is too speculative because: i) they have a great environmental plasticity, as many of them are Pontocaspian, ii) they often behave differently in the Pontocaspian area than in the rest of the world, and iii) some non-analogue situations to the modern surface samples existed in the past.

Recognising the limitations of using specific dinocyst types as indicators of specific salinity ranges, we have separated the dinocyst assemblages presented here in three broad groups (Table 2) according to not only their distribution in surface samples of the Pontocapian (Kazancı et al. 2004; Marret et al. 2004; Leroy et al. 2013a, 2013b, 2018; Mudie et al. 2017), but also to changes over time in sedimentary sequences (e.g. Dale 1996; Sorrel et al. 2006; Leroy et al. 2007, 2013c, 2014; Mudie et al. 2007; Marret et al. 2009). The three groups separate the following assemblages: *P. psilata-S. cruciformis-S. belerius* (Group 1), *I. caspienense* (Group 2) and *L. machaerophorum* and other taxa (Group 3) (Table 2). Group 1 would be indicative of fresher water environments in contraposition with Group 2, indicative of brackish waters. Group 3 includes the rest of the dinocysts.

Table 2: The three dinocyst groups separated according to salinity preference

Group	Taxa
1	*Pyxidinopsis psilata, Spiniferites cruciformis, Spiniferites belerius*
2	*Impagidinium caspienense*
3	*Lingulodinium machaerophorum* with all others*: Pentapharsodinium dalei* cyst*, Brigantedinium, Caspidinium rugosum, C. rugosum rugosum*

4 Results and interpretation of the new data

4.1 Base of core GS18

The additional 22 samples below 12.44 cal. ka BP in core GS18 show similar taxa to the already published upper part (Fig. SI 1, Leroy et al. 2014) with the dominance of *P. psilata*. Wide changes within the assemblages are, however, noted with especially high percentages in *Brigantedinium* and low dinocyst concentrations at 13.9-12.9 cal. ka BP, coeval to the Allerød oscillation.

4.2 Core Sh7

4.2.1 Lithology of core Sh7

A fine brown mud with black hydrotroilite layers (0.5 cm thick) characterises core Sh7 lithology from 600 to 423 cm, ending with a sharp transition. A fine oxidised mud with clear black hydrotroilite layers (2 cm thick)

with a progressive transition at its top characterises the 423-310 cm interval. From 310 to 230 cm, a light brown mud with hydrotroilite layers is evidenced. From 230 cm to the top, the core lithology is distinguished by a fine grey mud, more bedded at 230-175 and 115-20 cm depth. The grain size distribution analysis indicates very fine-grained sediment with a slight increase of the fine silt fraction at 137.5 cm (Fig. 2).

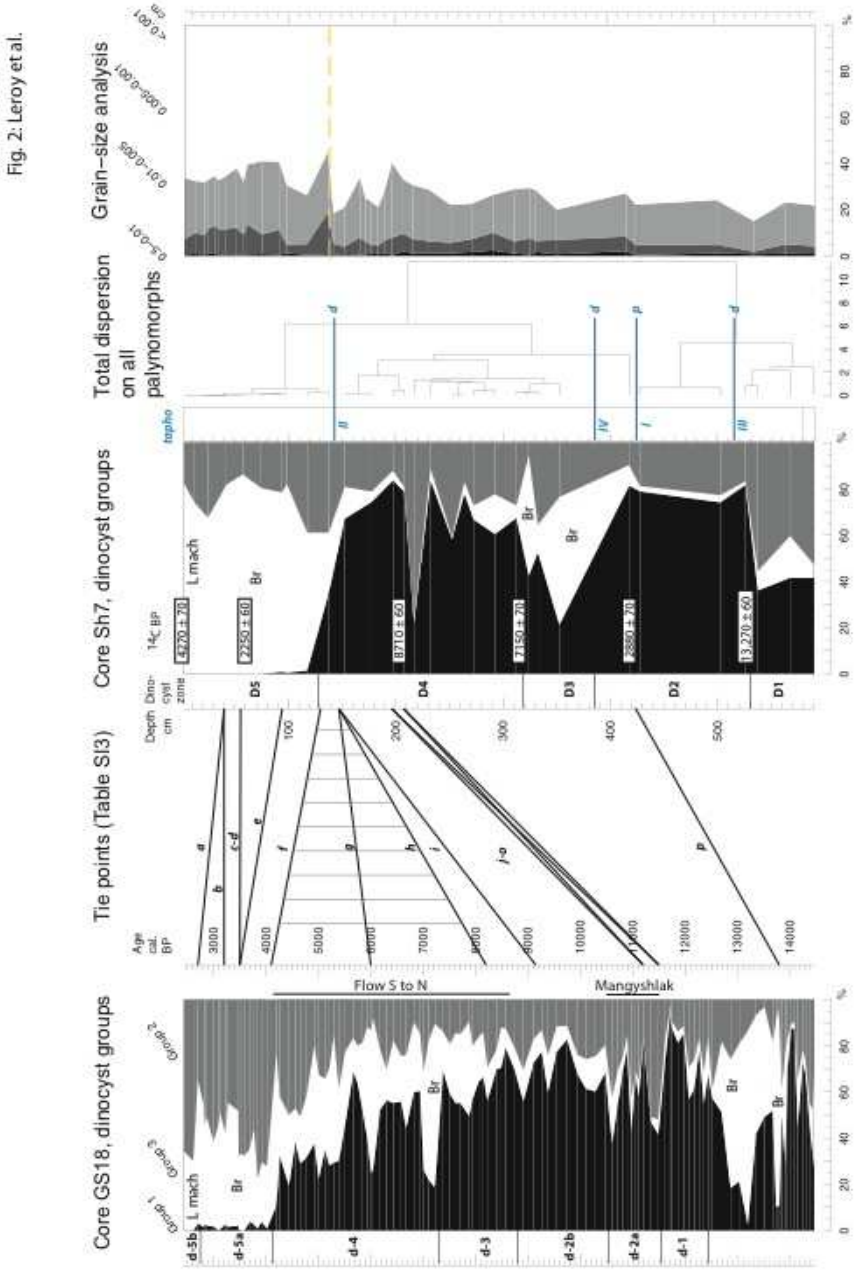

***Figure 2**: Comparison of the dinocyst synthetic records of the middle basin deep-water cores core GS18 and core Sh7 depicting the detected tie points (black lines) after comparing palynological records (more information in Table SI 3) to suggest*

a hypothetical chronological framework for core Sh7. Groups as in Table 2. The horizontal blue lines on core Sh7 are the four main taphonomical changes (tapho I to IV) (p = pollen, d = dinocyst) (SI 3). The dashed yellow line shows the main (and only) change in grain size for core Sh7, with a slight increase of the silty fraction. Br = Brigantedinium, L mach = Lingulodinium machaerophorum.

4.2.2 Zonation and interpretation of the Sh7 dinocyst record

The zonation performed on the dinocyst record of core Sh7 has allowed identifying five dinocyst zones (D1 to D5; Fig. 3). Zone D1 (590-532 cm) is dominated by *I. caspienense* (40-50%), with a significant representation of *P. psilata* (30-40%). The high *I. caspienense* values suggest an increase of salinity and point at a lowstand, the Enotaev or perhaps the Atelian according to different authors (Svitoch 2009, Yanina 2014).

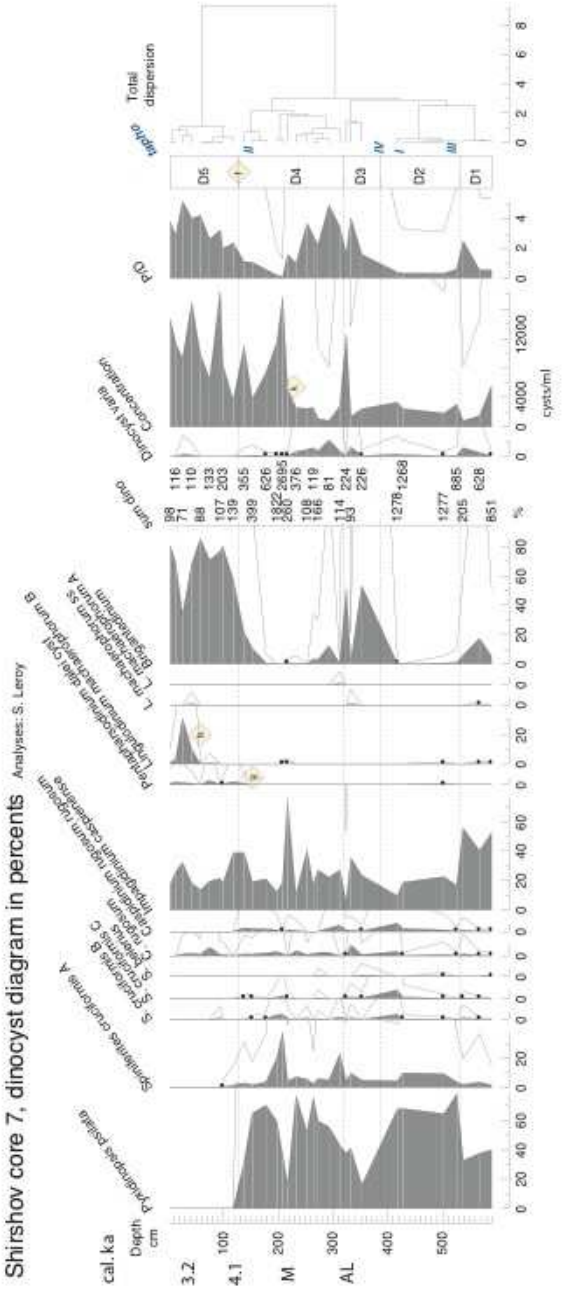

Figure 3*: Dinocyst diagram of core Sh7. Black dots indicate percentages lower than 0.5%. Dinocyst percentages are calculated on the sum of identified cysts, excluding varia. The zonation was performed by CONISS analysis after the square-root transformation of dinocyst percentages. M = Mangyshlak. Al = Allerød. Roman numbers in blue are indicative of taphonomical change (tapho I to IV) identified for the total palynological (pollen and dinocyst) record (SI 3). Letters in yellow lozenges are tie points (more information in Table SI 3).*

In zone D2 (532-385 cm), *P. psilata* dominates the assemblages (40-75%) followed by *I. caspienense* (10-20%). It has probably its equivalent in the first samples of core GS18 before 13.8 cal. ka BP (Fig. 2).

In zone D3 (385-318 cm), *P. psilata* values drop (15-40%) and *Brigantedinium* percentages increase significantly (5-55%). A similar phase of high *Brigantedinium* percentages is found at 13.8-12.8 cal. ka BP in core GS18, coeval with the end of the Allerød period (Fig. 2). The milder climate of the Allerød would have led to the melting of regional glaciers and permafrost (likely in the Greater Caucasus, Fig. 1) and, thus, leading to a greater in-wash of very fine particles into the CS. It is proposed that the CS waters became more turbid, so, less favourable to autotrophic phytoplankton, supporting heterotrophic species such as *Brigantedinium* (Garcia-Moreiras et al. 2018).

Zone D4 (318-127 cm) shows a noticeable drop in *Brigantedinium* percentages (0-25%), while the presence of *P. psilata* is maximal (up to 75%), except at 217-208 cm due to a single peak of *I. caspienense* at 217 cm followed by a single peak of *S. cruciformis* at 208 cm. It is also at 208 cm that the dinocyst concentration clearly increases. Zone D4 is equivalent to zones d-1and d-2 of core GS18, with the single peak of *I. caspienense* possibly representing the Mangyshlak.

Zone D5 (127-2.5 cm) is characterised by the disappearance of *P. psilata,* the quasi-disappearance of *S. cruciformis*, and the massive increase in *Brigantedinium* values (25-80%). *I. caspienense* retains similar values to the previous three zones. *P. dalei* cyst appears at the base of this zone, while *L. machaerophorum* at 42 cm. *C. rugosum rugosum*, that was previously present in low values, disappears. The main change in this diagram lies between zones D4 and D5 and it is the equivalent to the boundary of zones d-4 and d-5 of GS18.

4.2.3 Chronology of core Sh7

The details on how the chronological framework of core Sh7 has been built are found in Supplementary Information (SI 3a,b). A detailed pollen diagram is presented in SI 3a,b, as well as the explanation of the tie points deriving from it and from the dinocyst diagram. According to the tie points (Table SI3), 422 cm in depth would correspond to ~13.8 cal. ka BP, 200 cm to ~11.5-11.1 cal. ka BP, and 57.5 cm to ~3.5 cal. ka BP, with an identified sedimentary hiatus at 132 cm that would cover from ~9.2-8.2 to 4.1 cal. ka BP (Fig. 2).

5 Discussion

5.1 Salinity and water levels in the Caspian

Modellers have shown that the main drivers of CS levels, besides precipitation, are evaporation over the lake surface and river inflow (Arpe et al. 2007, 2012, 2014). Water level changes are, therefore, directly affecting water volume and dilution and, hence, salinity. Moreover, during highstands, overflows over the Manych Sill in the west and to the Karabogaz Gol in the east must have deprived the CS of salts (Fig.1; Leroy et al. in press). The link shown by biotic proxies between salinity, water volume and the water level is valid for the open water and clearly not for areas under delta influence (Leroy

et al. 2018). Indeed, the dinocyst groups and their changes over time are especially significant for deep waters. For example, Group 1 is not important in the coastal lagoon (core TM) in the post-regression early Holocene (Leroy et al. 2013a), because water is shallow and easily influenced by river mouth conditions, thus often displaying different salinities than in the open waters, i.e. higher or lower.

When **cumulative diagrams** are plotted displaying the three dinocyst groups considered in this work, the trends in Group 1 – that comprises dinocysts living at lower salinities – in comparison with the other two groups seem to indicate changes in water masses that could be construed as a qualitative indication of salinity trends (Fig. 4).

5.2 Dinocyst records from Caspian deep cores and comparison to previous water level reconstructions

The middle and south basin dinocyst records compiled here with dinocyst assemblages arranged in three groups by salinity preference reveal **five main environmental changes and a significant assemblage turnover** (Fig. 4).

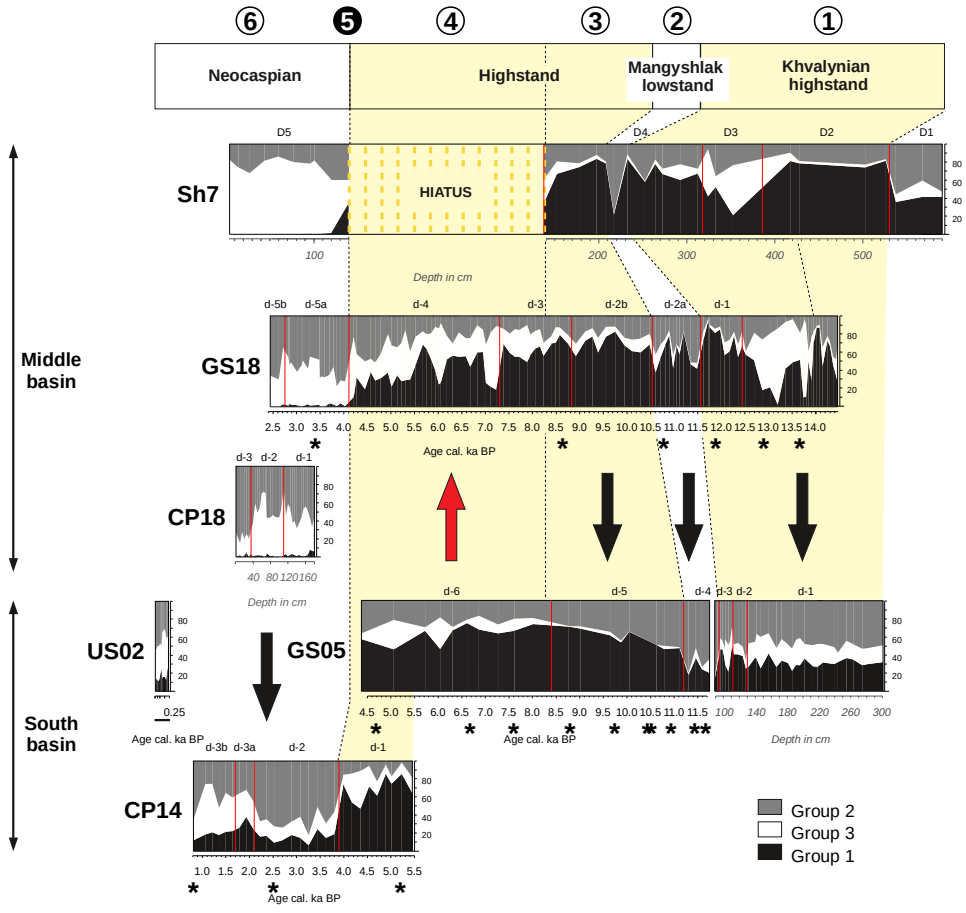

***Figure 4**: Dinocyst-inferred environmental changes after the compilation of the synthetic dinocyst records from the deep-water cores of the south (cores GS05, CP14 and US02) and middle (cores GS18, CP18, and Sh7) basins presented as cumulative curves of three environmental groupings (Table 2). Circled numbers at the top refer to the five main environmental phases and the significant assemblage turnover described in the text. Radiocarbon dates are indicated with asterisks and radionuclides by a bar.*

5.2.1 The Khvalynian highstand

The dominance of Group 1 over Group 2 in the dinocyst assemblages reconstructs high water levels at the end of the Pleistocene (phase 1, Fig. 4), in line with a highstand reconstructed by Varushchenko et al. (1987), Chepalyga (2007) and Svitoch (2009). This highstand has been related to the Khvalynian highstand. In addition, Group 1 also indicates that the salinity was low, as reconstructed by molluscs (Yanina 2014).

5.2.2 The Mangyshlak lowstand

A lowstand is reconstructed after the Khvalynian highstand, the so-called Mangyshlak (phase 2, Fig. 4). The chronology of this lowstand has been established at c. 11.5-10.5 cal. ka BP in the middle basin (Leroy et al. 2014), and at >11.7-11.2 cal. ka BP in the south basin (Leroy et al. 2013c) (Fig. 4). The time-span of the lowstand is reconstructed as longer in the northern shallow part of the CS using lithological and mollusc shells analyses, from 12 to 9 uncal. ka BP (Bezrodnykh and Sorokhin 2016). In addition to the changing CS levels, the larger importance of Group 2 indicates salinities higher than during the Khvalynian in the middle and south basins as (Fig. 4). In fact, this change in salinity is not only seen in the dinocyst records but also in an increase in the carbonate content in cores GS05 and GS18 (Leroy et al. 2013c, 2014), as well as in mollusc-based salinity reconstructions (Yanina 2014). It fits also the grain-size increase seen in multiple shallow and deep cores studied in the south and middle basins (e.g. Mayev 2010). However, it is quite remarkable that in close-by deep-water cores (cores SR12, GS04 and GS19), no clear Mangyshlak lowstand was highlighted after sedimentological and mineralogical studies (Kuprin et al. 2003).

5.2.3 The post-Mangyshlak highstand until 4 cal. ka BP

After the Mangyshlak lowstand up to c. 8.5-8.0 cal. ka BP, CS levels rose as depicted by the rise in the importance of Group 1 in the dinocyst records of the middle and south basins (phase 3, Fig. 4). The reconstructed highstand seems to have had similar features to the preceding Khvalynian in the middle basin, or even higher CS levels in the south basin. Based on sedimentological and mollusc analyses, this highstand period is either already called the Neocaspian (e.g. Yanina 2014) or still is the continuation of the Khvalynian highstand (e.g. Svitoch 2009, 2012), although never as high as the Pleistocene Khvalynian. It is not impossible that this highstand may have been previously confused with the glacial part of the Khvalynian, perhaps due to similarities of sediment or mollusc assemblages. Dinocyst assemblages show low salinity levels like those detected during the pre-Mangyshlak Khvalynian. Therefore, the dinocyst data would agree with some mollusc data in extending the Khvalynian biozone to this period, as the salinity suggested

for the Neocaspian is higher, thus reconstructing a period with different features than the Khvalynian ones (Svitoch 2009, 2012).

A small but significant shift in the salinity gradient is reconstructed from c. 8.5-8.0 to 4 cal. ka BP when comparing the dinocyst assemblages of the south and middle basins (phase 4, Fig. 4). After the Mangyshlak up to c. 8.5-8.0 cal. ka BP, the previously described phase, the freshwater is reconstructed flowing southwards, as today owing to the influence of the Volga River in the north. However, from such date and during four millennia, the water inflow seems to have reversed, as indicated by the larger importance of Group 1 in the south basin than in the middle basin. This means an unexpected-so-far south to middle basin water flow and the likely influence of rivers feeding the south basin. The turning point might have been the 8.2 cal. ka BP event that in the Caucasus meant a shift to wetter climate (Messager et al. 2013; Joannin et al. 2014). In addition to the wetter climate that existed in the Caucasus, several periods of low fluvial activity have been identified for the northern drainage of the CS, i.e. phase 6 from 8.5 to 5.5 ka b2k and phase 4 from 4.6 to 3.5 ka b2k (Panin and Matlakhova 2015). These relative dry periods would have decreased the flow of the Volga, impacting first the north and middle basins, and later the south basin.

With high levels in the CS, an overflow to the Black Sea is expected in this period, as it was the case for the Khvalynian highstand (Bahr et al. 2005). Hardly any trace of this is, however, known. Nevertheless, in the NE Black Sea (not far from the Azov Sea where the Don-Manych passage ends), a Holocene record shows that Mediterranean ostracod and dinocyst taxa are still co-existing with Caspian taxa at 7.4-6.8 cal. ka BP (Ivanova et al. 2015; Zenina et al. 2017). This may suggest a possible rather late inflow over the sill from the CS.

5.2.5 The 4 cal. ka BP shift

The sharpest change in the dinocyst assemblages is found at c. 4 cal. ka BP (phase 5, Fig. 4). This shift meant an assemblage turnover depicting a change in salinity from less brackish to more brackish dinocysts owing to the decline in Group 1. More specifically this shift has been detected at 3.9 cal. ka BP in the south basin (Leroy et al. 2007) and at 4.1 cal. ka BP in the middle basin (Leroy et al. 2014). This deep-water assemblage turnover, also seen in core Sh7 (Fig. 2 and 3), reflects an ecological threshold synchronous in the two basins (Fig. 2 and 4).

No obvious shift or event corresponding to the major dino-assemblage turnover at c. 4 cal. ka BP (around 3.7 ^{14}C ka BP) has been observed in previous CS level reconstructions (Leroy et al. in press). Nevertheless, a deep lowstand (>45 m bsl) is proposed in Svitoch (2009) around 4.2 ^{14}C ka BP. The lack of proxy evidence for an abrupt water level change four thousand years ago from other CS level reconstructions is perhaps owing to the relative abruptness of the shift, the composite nature of the published reconstructions, and their limited chronological control (Leroy et al. in press). In core Sh7, the shift is expressed by an event causing the loss of underlying sediment (Fig. 2). The shift is coeval to a distinctive gypsum level in the lagoonal core TM related thus to the culmination of a significant local drop of the water level at 7.6 to 4 cal. ka BP (Leroy et al. 2013a; Kakroodi et al. 2015). Moreover, it is intriguing that in the fluvial activity reconstruction of the East European plain

(i.e. Volga drainage basin), a period with low activity occurs at that point (fluvial phase 4 of Panin and Matlakhova 2015). A possible link with the 4.2 cal. ka BP drought event seen in the Iranian central Plateau (Schmidt et al. 2007) has been proposed and discussed earlier (Leroy et al. 2014).

5.2.6 The Neocaspian period

Finally, from c. 4 cal. ka BP onwards the dinocyst records show larger importance of Group 2 in the assemblages (phase 6, Fig. 4). This period, that is not reconstructed as a highstand due to the low values of Group 1, but also seems to have been a lowstand owing to the large importance of Group 2, is the Neocaspian period.

5.2.7 Other features of the dinocyst records

There are some other features in the dinocyst records that are worth mentioning. Increases of *Brigantedinium* in the Allerød in cores GS18 and Sh7 (middle basin), and some later ones (Fig. SI 1), are probably nutrient-driven owing to the ecology of this dinocyst (García-Moreiras et al. 2018). So far, no clear evidence of an increase in water surface temperature can be seen in the dinocyst assemblages apart from the recent expansion of *L. machaeorophorum* (Leroy et al. 2013b), although water surface temperature is likely to have played a considerable role since the LGM. The progressive increase in biological carbonate content typical of the Mangyshlak lowstand could reflect this temperature increase by allowing plankton to bloom more readily (Mayev 2010; Leroy et al. 2013c).

Most of the CS level reconstructions are from shallow facies and many show more fluctuations than the dinocyst reconstruction. It is very likely that the simpler scheme of water level presented here in comparison to the *more complex previous reconstructions* based on sedimentology and mollusc assemblages (e.g. Svitoch 2012) is caused by a buffering due to the water depth and the distance to the shores. It is most likely that only the largest water level fluctuations are recorded in the deep basins. Alternatively, the previously reconstructions made using the data from many different locations are not stacked together in a clean chronological succession. Moreover, most of the sites used to build the available water-level reconstructions derive from coastal locations where regression or transgression might have been felt earlier or later than in deep locations. A good example of this is the Mangyshlak duration of c. 1000 years in the deep cores from the south and middle basins (Fig. 4) versus several-millennia-long lowstand in cores located closer to the north basin margin (Bezrodnykh and Sorokhin 2016).

5.3 N-S salinity gradient between the Caspian Sea basins

An interesting feature appears when comparing the dinocyst records from the middle and south basins (Fig. 4). Most of the reconstructed salinities (phases 1, 2, 3 and 6) reflect a southwards flow, meaning an increase in salinity from north to south. This feature is in line with the current hydrological status of the CS, in which the southwards flow is the result of the prominence of Volga River discharge in the north basin. However, the typical southwards flow seems to have shifted from 8.5-8.0 to c. 4 cal. ka BP (phase 4), when a northwards flow is reconstructed from the south to the middle basin (Fig. 4).

This four-millennia-long shift could be due to lower evaporation in the south basin or, most likely, owing to a change in the hydrography.

Long-term changes in the hydrography have already been suggested for the CS. The meridional flow direction seems to have changed several times in the past as shown by the study of bottom sediments in the Apsheron Sill (Fig. 1) between the middle and the south basin (Ferronsky et al. 1999). Moreover, the fresh morphology of the trench and the sediment structure in cores taken in the sill itself support periods of changing flow direction between basins (Kuprin 2002). These two investigations have indicated that, on several occasions, a significant freshwater inflow came from the melting of southern highland glaciers. Unfortunately, the timeframes of the changes in flow direction remained undated.

5.4 Freshwater sources

The fluvial activity in the East European Plain, including the Volga River, is reconstructed as very strong during the late Pleistocene, from 18 to 11.7 ka b2k. In comparison, the Holocene experienced a much lower fluvial activity (Panin and Matlakhova 2015). Moreover, the Eurasian ice sheet had already withdrawn from the Volga drainage basin by 13.8 cal. ka BP (Tudryn et al. 2016).

According to the long-term dinocyst records, it seems that for most of the last fourteen millennia the water flowed from the middle to the south basin indicating an influence from the Volga River freshwater discharge, as it happens nowadays. However, the water flow for the 8.5-8.0 to 4 cal. ka BP interval (phase 4, Fig. 4) is reconstructed as reversed from the southward general pattern, indicating an additional and voluminous inflow of freshwater from the south basin. Two lines of thoughts are discussed to explain the source of fresh water: on the one hand the climate in the Karakum desert (Turkmenistan), i.e. the area between the CS and the Amu-Darya (Fig. 1), and on the other hand the flow of the Amu-Darya River. In sum, pluvial and fluvial explanations.

5.4.1 The early and mid-Holocene climate in the Karakum

The pollen assemblages trapped in deep-water sediments are overrepresented by pollen types wind-transported over long distances, thus reflecting part of the drainage basin of the CS. The drainage basin area better represented is likely to be the westwards of it owing to dominant winds at the time of peak pollen production (Leroy et al. 2007). The climate at the Holocene onset is reconstructed as very dry around the CS according to pollen records from the middle and south basins (Leroy et al. 2013c, 2014). The development of a long phase whose vegetation was characterised by steppic bushes is noted at c. 11.5-8.4 cal. ka BP in the south basin, and at c. 11.4-8.2 cal. ka BP in the middle basin, with the tree expansion that usually characterises the Holocene onset starting progressively after 8.4-8.2 cal. ka BP only (Leroy et al. 2013c, 2014). Therefore, it is only from c. 8.4-8.2 cal. ka BP that the climate around the middle and south CS basins became slightly more humid.

This observation fits rather well with a “pluvial” phase, the Liavliakan phase, reconstructed for the south-eastern Caspian area at c. 8.8-4.5 cal. ka BP

(published as 8 to 4 ^{14}C ka BP), peaking at c. 7.5 cal. ka BP (published as 6.5 ^{14}C ka BP) in the Karakum desert (mainly Turkmenistan, Fig. 1) (Lioubimtseva et al. 1998). This more humid period had been suggested also in previous palaeoenvironmental studies in the nearby Aral Sea (Breckle and Geldyeva 2012). In addition, archaeological research and dune geomorphology evidence indicate that Turkmenistan and central Asia were wetter for a few thousand years before c. 5.5-4.5 cal. ka BP (published as 5 or 4 ^{14}C ka BP) (Kes and Klyukanova 1990; Lioubimtseva et al. 1998; Maman et al. 2011). Around 4000 years ago, populations living at the foot of the Kopet-Dag, at the south-eastern of the CS (Fig. 1), left the area. This migration was likely the result of the decrease in the mountainous river flow, forcing the populations to live in the plain in the large deltas, such as in the Murghab Delta (Masson 1992).

5.4.2 The flow of the Amu-Darya and distant influence from the Himalayas

Ferronsky et al. (1999) have suggested that the source of water for this reversed salinity gradient is in the glaciers from southern slopes of the drainage basin. The freshwater would be most likely coming from the Amu-Darya via the now-defunct Uzboy River, a distributary of the Amu-Darya (Leroy et al. 2007). Therefore, the freshwater would derive from the Pamir and Hindu-Kush regions (Fig. 1). However, no direct evidence has been found for that source.

In geological and historical times, the Uzboy acted as the lower reaches of the Amu-Darya. In fact, it even seems that the most common flow of the Amu-Darya over the last million years has been to the CS rather than to the Aral Sea (Létolle 2000). The Amu-Darya was then located further S-W and was following the foothill of the Kopet-Dag (Létolle 2000). In the Pliocene, a large delta formed at its mouth in the eastern part of the south basin (Torres 2007). In the Quaternary, the Uzboy and Amu-Darya often drained in the CS (Kes and Klyukanova 1990; Ferronsky et al. 1999; Létolle 2000). However, in the late Quaternary, the Amu-Darya was increasingly deviated towards the Aral Sea due to tectonic movements (Létolle 2000; Hollingsworth et al. 2010). From the Holocene onset to c. 5.8 cal. ka BP (published as c. 5 ^{14}C ka BP), the Amu-Darya was either directly flowing to the CS via the Uzboy and/or the Sarykamish (a lake between the Aral and the CS), or it was so powerful during The Great Aral Phase that the Aral Sea waters flew over to the CS still via the Uzboy and Sarykamish (Boomer et al. 2000; Breckle and Geldyeva 2012). These authors justify the large water volume for that period as derived from the Liavliakan pluvial period causing an increased river flow in the Amu-Darya and Syr-Darya. In the late Holocene, it is known from historical accounts that people were able to destroy irrigation dams on the Amu-Darya, e.g. in the region of Urgench, to turn its flow to the CS (Kes and Klyukanova 1990; Naderi et al. 2013; Krivonogov et al. 2014; Haghani et al. 2016).

Therefore, it is very likely that the Amu-Darya flew in the CS from c. 8.5 to 4 cal. ka BP, partially fed by i) the Liavliakan humid period, and ii) by waters coming from an area with a climatic regime completely different from the regime over the Volga drainage basin (Fig. 1). Hydrographers have shown that a positive correlation exists between the modern flow of the Amu-Darya and peaks of the Indian Summer Monsoon (Schiemann et al. 2007). This is currently via an increase of glacier melting due to temperature rise, not by

direct increase of monsoonal precipitation. However, the early Holocene situation was different, as the Indian Summer Monsoon was stronger (Wanner et al. 2008; Owen 2009) and hence might have overflown into the Amu-Darya drainage basin. In parallel, the Indian Summer Monsoon decreased around the 4.2 cal. ka BP event (Staubwasser et al. 2003), and this may have caused a decrease in the flow of the Amu-Darya via a direct decrease in precipitation on its headwaters or via a decrease of the glacier melting in its headwaters (Schiemann et al. 2007).

Finally, the change of the Amu-Darya flow to the Aral Sea after the c. 8.5-4 cal. ka BP interval is likely due to the local climate in the Karakum and climate upstream where the glaciers are located. The deviation of the Amu-Darya from the CS to the Aral Sea may have been caused by i) shifting sand dunes in the Karakum desert (where the Amu-Darya turns west to the CS) that are frequent and whose activity could easily have been intensified by the 4.2 cal. ka BP event with its 300 year long drought (Kaniewski et al. 2018); and ii) one of the many tectonic movements in the Amu-Darya lower basin (Hollingsworth et al. 2010; Crétaux et al. 2013).

6 Conclusions

The long-term dinocyst records from three deep-water sedimentary sequences located in the middle and south CS basin have revealed 1) an early Holocene lowstand (Mangyshlak), 2) high water levels in the first half of the Holocene, just after the Mangyshlak lowstand, and 3) a dinocyst assemblage turnover at 4 cal. ka BP.

In addition, disrupting the southwards surface water flow that characterises the CS nowadays and most of the last fourteen millennia, a reversed surface water flow (northwards) is reconstructed during the second half of the post-Mangyshlak highstand, from 8.5-8.0 to 4 cal. ka BP. This reversed water flow should be linked to a southern source of water. The southern source of water is most likely explained by a more humid climate in the Karakum and a strong outflow of the Amu-Darya, pointing at the Amu-Darya bringing meltwaters from the Indu-Kush and Pamir to the CS.

Still, other proxies remain to be explored that would aid to solve the water-level conundrum and suit the idiosyncrasies of the CS. This would help to identify the precise source of water during the Holocene. In this respect, neodymium (Tudryn et al. 2016) and strontium (Pierret et al. 2012) isotopes seem promising.

Finally, regarding the factors driving the CS level, we agree with Kes and Klyukanova (1990) that the role of rivers is vastly underestimated in the Pontocaspian region.

Acknowledgements

The samples from core Sh7 have been kindly provided by A. Roslyakov, V. Putans, and E. Novichkova (Shirshov Institute of Oceanology, Russia). The late V.N. Lukashin (SIO) is especially acknowledged for his contribution to the fieldwork, sampling and geological aspects of core Sh7 investigation. Expeditionary research and partial sample preparation were obtained in the framework of the state assignment of FASO Russia (theme № 0149-2019-0007). We are grateful to G. Bayon and S. Toucanne (IFREMER, France) who covered the costs of the six radiocarbon dates of core Sh7, and to S.

Kroonenberg (University of Delft, The Netherlands) for thought-provoking discussions. We are also grateful to the two anonymous reviewers, who provided positive, constructive feedback to a previous version of the manuscript. This publication is a contribution to the European project Marie Curie, CLIMSEAS-PIRSES-GA-2009-247512. Declarations of interest: none.

References

Arpe, K., Leroy, S.A.G., 2007. The Caspian Sea Level forced by the atmospheric circulation, as observed and modelled. Quaternary International 173-174, 144-152.

Arpe, K., Leroy, S.A.G., Lahijani, H., Khan, V., 2012. Impact of the European Russia drought in 2010 on the Caspian Sea level. Hydrology and Earth System Science 16, 19-27.

Arpe, K., Leroy, S.A.G., Wetterhall, F., Khan, V., Hagemann, S., Lahijani, H., 2014. Prediction of the Caspian Sea Level using ECMWF seasonal forecast and reanalysis. Theoretical and Applied Climatolog, 117, 41-60.

Arpe, K., Tsuang, B.-J., Tseng, Y.-H., Liu, X.-Y., Leroy, S.A.G., 2018. Quantification of climatic feed-backs on the Caspian Sea Level variability and impacts from the Caspian Sea on the large scale atmospheric circulation. Theoretical and Applied Climatology 14 pages.

Arslanov, K.A., Yanina, T.A., Chepalyga, A.L., Svitoch, A.A., Makshaev, F.E., Maksimov, S.B., Chernov, N.I., Tertychniy, A.A., 2016. On the age of the Khvalynian deposits of the Caspian Sea coast according to ^{14}C and $^{230}Th/^{234}U$ methods. Quaternary International 409, 81– 87.

Bahr, A., Lamy, F., Arz, H., Kuhlmann, H., Wefer, G., 2005. Late glacial to Holocene climate and sedimentation history in the NW Black Sea. Marine Geology 214: 309– 322.

Bezrodnykh, Y.P., Sorokhin, V.M., 2016. On the age of the Mangyshlakian deposits of the northern Caspian Sea. Quaternary Research, 85: 245-254.

Boomer, I., Aladin, N., Plotnikov, I., Whatley, R., 2000. The palaeolimnology of the Aral Sea: a review. Quaternary Science Reviews 19, 1259-1278.

Boomer, I., von Grafenstein, U., Guichard, F., Bieda, S., 2005. Modern and Holocene sublittoral ostracod assemblages (Crustacea) from the CS: a unique brackish, deep-water environment. Palaeogeography, Palaeoclimatology, Palaeoecology 225, 173-186.

Breckle, S.-W., Geldyeva, G.V., 2012. Dynamics of the Aral Sea in Geological and Historical Times. Chap 2. *In* Aralkum - a Man-Made Desert: The Desiccated Floor of the Aral Sea (Central Asia). Breckle, S.-W., et al. (Eds.) Ecological Studies 218, DOI 10.1007/978-3-642-21117-1_2, Springer-Verlag Berlin Heidelberg. pp. 13-35.

Cazenave, A., Bonnefond, P., Dominh, K., Schaeffer, P., 1997. Caspian sea level from TOPEX/POSEIDON altimetry: level now falling. Geophysical Research Letters 24, 881–884.

Chalié, F., and the Caspian Sea INSU-DYTEC Program Members: Escudié, A.S., Badaut-Trauth, D., Blanc, G., Blanc-Valleron, M.M., Brigault, S., Desprairies, A., Ferronsky, V.I., Giannesini, P.J., Gibert, E., Guichard, F., Jelinowska, A., Massault, M., Mélières, F., Tribovilllard, N., Tucholka, P., Gasse, F., 1997. The glacial-post glacial transition in the southern Caspian Sea. Comptes Rendus de l'Académie des Sciences Paris, série 2a 324, serie IIa, 309-316.

Chepalyga, A.L., 2007. The late glacial great flood in the Ponto-Caspian basin. *In* The Black Sea Flood Question. *Edited by* V. Yanko-Hombach, A.S. Gilbert, N. Panin, and P.M. Dolukhanov. Dordrecht, Springer. pp. 119-148.

Cohen, A.S., Stone, J.R., Beuning, K.R.M., Park, L.E., Reinthal, P.N., Dettman, D., Scholz, C.A., Johnson, T.C., King, J.W., Talbot, M.R., Brown, E.T., Ivory, S.J., 2007. Ecological consequences of early Late Pleistocene megadroughts in tropical Africa. Proceedings National Academy of Science 104, 16422–16427.

Colman, S.M., Karabanov, E.B., Nelson, Iii, C.H., 1993. Quaternary sedimentation and subsidence history of Lake Baikal, Siberia, based on seismic stratigraphy and coring. USGS Staff -- Published Research. Paper 279. http://digitalcommons.unl.edu/usgsstaffpub/279.

Crétaux J.-F., Létolle R., Bergé-Nguyen M., 2013. History of Aral Sea level variability and current scientific debates. Quaternary International 110, 99-1113.

Dale, B., 1996. Dinoflagellate cyst ecology: modelling and geological applications. *In* Palynology: Principles and Applications. Jansonius, J., McGregor, D.C. (Eds.). Vol. 3. American Association of Stratigraphic Palynologists Foundation. pp. 1249– 1275.

Ellegaard, M., Lewis, J., Harding, I., 2002. Cyst-theca relationship, life cycle, and effects of temperature and salinity on the cyst morphology of *Gonyaulax baltica* sp. nov. (Dinophyceae) from the Baltic Sea area. Journal of Phycology 38, 775–789.

Ferronsky, V.I., Polyakov, V.A., Kuprin, P.N., Lobov, A.L., 1999. The Nature of the Fluctuation of Caspian Sea Level (Based on Results of the Study of Bottom Sediments). Water Resources 26, 6, 652–666.

García-Moreiras, I., Pospelova, V., García-Gil, S., Muñoz Sobrino, C., 2018. Climatic and anthropogenic impacts on the Ría de Vigo (NW Iberia) over the last two centuries: A high-resolution dinoflagellate cyst sedimentary record. Palaeogeography, Palaeoclimatology, Palaeoecology 504, 201–218.

Gebhardt, A.C., Naudts, L., De Mol, L., Klerkx, J., Abdrakhmatov, K., Sobel, E. R., De Batist, M., 2017. High-amplitude lake-level changes in tectonically active Lake Issyk-Kul (Kyrgyzstan) revealed by high-resolution seismic reflection data. Climate of the Past 13, 73–92.

Haghani, S., Leroy, S.A.G, Khdir, S., Kabiri, K, Naderi Beni, M., Lahijani, H.A.K., 2016. An early Little Ice Age brackish water invasion along the coast of the Caspian Sea (sediment of Langarud wetland) and its wider impacts on the environment and people. The Holocene 26, 3-16.

Hollingsworth, J., Fattahi, M., Walker, Ri., Talebian, M., Bahroudi, A., Bolourchi, M.J., Jackson, J., Copley, A., 2018. Oroclinal bending, distributed thrust and strike-slip faulting, and the accommodation of Arabia–Eurasia convergence in NE Iran since the Oligocene. Geophysical Journal International 181, 1214–1246.

Ivanova, E.V., Marret, F., Zenina, M.A., Murdmaa, I.O., Chepalyga, A.L., Bradley, L.R., Schornikov, E.I., Levchenko, O. V., Zyryanova, M.I., 2015. The Holocene Black Sea reconnection to the Mediterranean Sea: New insights from the northeastern Caucasian shelf. Palaeogeography, Palaeoclimatology, Palaeoecology 427, 41–61.

Joannin, S., Ali, A. A., Ollivier, V., Roiron, P., Peyron, O., Chevaux, S., Nahapetyan, S., Tozalakyan, P., Karakhanyan, A., Chataigner, C., 2014. Vegetation, fire and climate history of the Lesser Caucasus: a new Holocene record from Zarishat fen (Armenia). Journal of Quaternary Science 29/1, 70-82.

Kakroodi, A.A., Kroonenberg, S.B., Hoogendoorn, R.M., Mohammadkhani, H., Yamani, M., Ghassemi, M.R., Lahijani, H.A.K., 2012. Rapid Holocene sea-level changes along the Iranian Caspian coast. Quaternary International 263, 3–103.

Kakroodi, A.A., Leroy, S.A.G., Kroonenberg, S.B., Lahijani, H.A.K., Alimohammadian, H., Boomer, I., Goorabi, A., 2015. Late Pleistocene and Holocene sea-level change and coastal palaeoenvironment along the Iranian Caspian shore. Marine Geology 361, 111-125.

Kaniewski, D., Marriner, N., Cheddadi, R., Guiot, J., Van Campo, E., 2018. The 4.2 ka BP event in the Levant. Clim. Past 14, 1529–1542.

Kazancı, N., Gulbabazadeh, T., Leroy, S.A.G., Ileri, O., 2004. Sedimentary and environmental characteristics of the Gilan-Mazenderan plain, northern Iran: influence of long- and short-term Caspian water level fluctuations on geomorphology. Journal of Marine Systems 46, 145-168.

Kes, A.S., Klyukanova, I. A., 1990. Causes of Aral Sea level variations in the past (in Russian). Izvestiya Akadernii Nauk SSSR, seriya geograficheskuya 1, 78-86.

Klige, R.K., 1990. Historical changes of the regional and global hydrological cycles. Geo-journal 20.2, 129-136.

Kostianoy, A., Kosarev, A., 2005. The Caspian Sea environment. Springer, Berlin-Heidelberg.

Krivonogov, S.K., Burr, G.S., Kuzmin, Y.V., Gusskov, S.A., Kurmanbaev, R.K., Kenshinbay, T.I., Voyakin, D.A., 2014. The fluctuating Aral Sea: A multidisciplinary-based history of the last two thousand years. Gondwana Research 26, 284–300.

Kuprin, P.N., 2002. Apsheron Threshold and Its Role in the Processes of Sedimentation and Formation of Hydrological Regimes in the Southern and Middle Caspian Basins. Water Resources 29, 5, 473–484.

Kuprin, P.N., Ferronsky, V.I., Popovchak, V.P., Shlykov, V.G., Zolotaya, L.A., Kalisheva, M.V., 2003. Bottom sediments of the Caspian Sea as an indicator of changes in its water regime. Water Resources 30 (2), 136-153.

Lahijani, H., Abbasian, H., Naderi–Beni, A., Leroy, S.A.G., Habibi, P., Haghani, S., Hosseindust, M., Shahkarami, S., Yeganeh, S., Zandi, Z., Tavakoli, V., Azizpour, J., Sayed-Valizadeh, M., Pourkerman, M., Shah-Hosseini, M., in press. Distribution pattern of South Caspian Sea sediment. Canadian Journal of Earth Sciences.

Lahijani, H.A.K., Naderi Beni, A., Kazanci, N., Gürbüz, A., Leroy, S.A.G., 2016. Editorial: Rapidly changing large lakes and human response *“QuickLakeH”*. Quaternary International 108, 1-15.

Leroy, S.A.G., Kakroodi, A.A., Kroonenberg S.B., Lahijani H.A.K., Alimohammadian H., Nigarov A., 2013a. Holocene vegetation history and sea level changes in the SE corner of the Caspian Sea: relevance to SW Asia climate. Quaternary Science Reviews 70, 28-47.

Leroy, S.A.G., López-Merino, L., Tudryn, A., Chalié, F., Gasse, F., 2014. Late Pleistocene and Holocene palaeoenvironments in and around the Middle

Caspian Basin as reconstructed from a deep-sea core. Quaternary Science Reviews 101, 91-110.
Leroy, S.A.G., Lahijani, H.A.K., Reyss, J.-L., Chalié, F., Haghani, S., Shah-Hosseini, M., Shahkarami, S., Tudryn, A., Arpe, K., Habibi, P., Nasrollahzadeh, H.S., Makhlough, A., 2013b. A two-step expansion of the dinocyst *Lingulodinium machaerophorum* in the Caspian Sea: the role of changing environment. Quaternary Science Reviews 77, 31-45.
Leroy, S.A.G., Marret, F., Giralt, S., Bulatov, S.A., 2006. Natural and anthropogenic rapid changes in the Kara-Bogaz Gol over the last two centuries by palynological analyses. Quaternary International 150, 52-70.
Leroy, S.A.G., Marret, F., Gibert, E., Chalié, F., Reyss, J.-L., Arpe, K., 2007. River inflow and salinity changes in the Caspian Sea during the last 5500 years. Quaternary Science Reviews 26, 3359-3383.
Leroy, S.A.G., Tudryn, A., Chalié, F., López-Merino, L., Gasse, F., 2013c. From the Allerød to the mid-Holocene: palynological evidence from the south basin of the Caspian Sea. Quaternary Science Reviews 78, 77-97.
Leroy, S.A.G., Chalié, F., Wesselingh, F., Sanjani, S., Lahijani, H.A.K., Athersuch, J., Struck, U., Plunkett, G., Reimer, P.J., Habibi, P., Kabiri, K., Haghani, S., Naderi Beni, A., Arpe, K., 2018. Multiproxy indicators in a Pontocaspian system: a depth transect of surface sediment in the S-E Caspian Sea. Geologica Belgica 21, 3-4, 143-165.
Leroy, S.A.G., Lahijani, H., Crétaux, J.-F., Aladin, N., Plotnikov, I., in press. Past and current changes in the largest lake of the world: The Caspian Sea. In: Mischke S. (ed.) Large Asian lakes in a changing world. Springer
Létolle, R., 2000. Histoire de l'Ouzboï, cours fossile de l'Amou Darya synthèse et éléments nouveaux. Studia Iranica 29 (2), 195-240.
Lewis, J., Taylor, J., Neale, K., Leroy, S.A.G., 2018. Expanding known dinoflagellate distributions: Investigations of slurry cultures from Caspian Sea sediment. Botanica Marina 61(1), 21–31.
Lioubimtseva, E., Simon, B., Faure, H., Faure-Denard, L., Adams, J.M., 1998. Impacts of climatic change on carbon storage in the Sahara-Gobi desert belt since the late glacial maximum. Global Planetary Change 16–17, 95–105.
Makshaev, R.R., Svitoch, A.A., Yanina, T.A., Badyukova, E.N., Khomchenko, D.S., Oshchepkov, G.V., 2015. Lower Khvalynian sediment record of the middle and lower Volga region. GCP 610 Third Plenary Conference and Field Trip, Astrakhan, Russia, 22-30 September, 2015, pp. 126-128.
Maman, S., Tsoar, H., Blumberg, D.G., Porat, N., 2011. Aeolian mobility and stability of the central Asian ergs, a study by remote sensing and geographic information systems. ISPRS Archive Vol. XXXVIII, Part 4-8-2-W9.
Mamedov, A.V., 1997. The Late Pleistocene-Holocene history of the Caspian Sea. Quaternary International 41-42, 161-166.
Marret, F., Leroy, S., Chalié, F., Gasse, F., 2004. New organic-walled dinoflagellate cysts from recent sediments of central Asian seas. Review of Palaeobotany and Palynology 129, 1–20.
Marret, F., Mudie, P., Aksu, A., Hiscott, R.N., 2009. A Holocene dinocyst record of a two-step transformation of the Neoeuxinian brackish water lake into the Black Sea. Quaternary International 197, 1-2, 72-86.

Masson, V.M., 1992. The decline of the Bronze Age civilization and movements of the tribes. *In* History of civilisations of Central Asia. Dani, A.H. and Masson, V.M. (Eds.). UNESCO Publishing, Paris, Vol. 1, pp. 326-345.

Mayev, E.G., 2010. Mangyshlak regression of the Caspian Sea: relationship with climate. *In* Proceedings of the International Conference —The Caspian Region: Environmental Consequences of the Climate Change. October, 14–16, Moscow, Russia. Moscow: Faculty of Geography, pp. 107-109.

Mertens, K., Ribeiro, S., Bouimetarhan, I., Caner, H., Combourieu-Nebout, N., Dale, B., de Vernal, A., Ellegaard, M., Filipova, M., Godhe, A., Grøsfjeld, K., Leroy, S.A.G., co-authors, 2009. Process length variation in cysts of a dinoflagellate, *Lingulodinium machaerophorum*, in surface sediments: investigating its potential as salinity proxy. Marine Micropalaeontology 70, 54-69.

Mertens, K.N., Takano, Y., Gu, H.F., Bagheri, S., Pospelova, V., Pieńkowski, A., Leroy, S.A.G., Matsuoka, K., 2017. Cyst-theca relationship and phylogenetic position of *Impagidinium caspienense* incubated from Caspian Sea surface sediments: evidence for heterospory within gonyaulacoid dinoflagellates. Journal of Eukaryotic Microbiology 64 (6), 829-842.

Messager, E., Belmecheri, S., Von Grafenstein, U., Nomade, S., Ollivier, V., Voinchet, P., Puaud, S., Courtin-Nomade, A., Guillou, H., Mgeladze, A., Dumoulin, J.P., Mazuy, A., Lordkipanidze D., 2013. Late Quaternary record of the vegetation and catchment-related changes from Lake Paravani (Javakheti, South Caucasus). Quaternary Science Reviews 77, 125-140.

Mudie, P.J., Marret, F., Aksu, A.E., Hiscott, R.N., Gillespie, H., 2007. Palynological evidence for climatic change, anthropogenic activity and outflow of Black Sea Water during the late Pleistocene and Holocene: centennial- to decadal-scale records from the Black and Marmara Seas. Quaternary International 167-168, 73-90.

Mudie, P., Marret, F., Mertens, K., Shumilovikh, L., Leroy, S.A.G., 2017. Atlas of modern dinoflagellate cyst distributions in the Black Sea Corridor, including Caspian and Aral Seas. Marine Micropaleontology 134, 1-152.

Naderi Beni, A., Lahijani, H., Mousavi Harami, R., Arpe, K., Leroy, S.A.G., Marriner, N., Berberian, M., Ponel, V.A., Djamali, M., Mahboubi, A., Reimer, P.J., 2013. Caspian sea level changes during the last millennium: historical and geological evidences from the south Caspian Sea. Climate of the Past 9, 1645-1665.

Owen, L.A., 2009. Latest Pleistocene and Holocene glacier fluctuations in the Himalaya and Tibet. Quaternary Science Reviews 28, 2150–2164.

Panin, A., Matlakhova, E., 2015. Fluvial chronology in the East European Plain over the last 20 ka and its palaeohydrological implications. Catena 130, 46–61.

Petelin, V.P., 1967. Granulometric analysis of the marine bottom sediments. Moscow Nauka. 125 pp

Pierret, M.C., Chabaux, F., Leroy, S.A.G., Causse, C., 2012. A record of Late Quaternary continental weathering in the sediment of the Caspian Sea:

evidence from U-Th, Sr isotopes, trace element and palynological data. Quaternary Science Reviews 51, 40-55.
Richards, K., Bolikhovskaya, N.S., Hoogendoorn, R.M., Kroonenberg, S.B., Leroy, S.A.G., Athersuch, A., 2014. Reconstructions of deltaic environments from Holocene palynological records in the Volga delta, northern Caspian Sea. The Holocene 24 (10), 1226-1252.
Rychagov, G.I., 1997. Holocene oscillations of the Caspian Sea, and forecasts based on palaeogeographical reconstructions. Quaternary International 41/42, 167–172.
Schiemann, R., Glazirina, M.G., Schär, C., 2007. On the relationship between the Indian summer monsoon and river flow in the Aral Sea basin. Geophysical Research Letters, 34, L05706.
Schmidt, A., Quigley, M., Fattahi, M., Azizi, G., Maghsoudi, M., Fazeli, H., 2011. Holocene settlement shifts and palaeoenvironments on the Central Iranian Plateau: investigating linked systems. Holocene 21 (4), 583-595.
Shumilovskikh, L.S., Fleitmann, D., Nowaczyk, N.R., Behling, H., Marret, F., Wegwerth, A., Arz, H.W., 2014. Orbital- and millennial-scale environmental changes between 64 and 20 ka BP recorded in Black Sea sediments. Climate of the Past 10, 939–954.
Sorrel, P., Popescu, S.-M., Head, M.J., Suc, J.P., Klotz, S., Oberhänsli, H., 2006. Hydrographic development of the Aral Sea during the last 2000 years based on a quantitative analysis of dinoflagellate cysts. Palaeogeography, Palaeoclimatology, Palaeoecology 234, 2–4, 304-327.
Staubwasser, M., Weiss, H., 2006. Holocene climate and cultural evolution in late prehistoric early historic West Asia - introduction. Quaternary Research 66 (3), 372-387.
Svalnov V.N., Kazarina G. Kh., 2008. Diatomaceous Oozes of the Middle Caspian Sea. Oceanology 48 (4), 588–594.
Svitoch, A.A., 2009. Khvalynian transgression of the Caspian Sea was not a result of water overflow from the Siberian Proglacial lakes, nor a prototype of the Noachian flood. Quaternary International 197, 115–125.
Svitoch, A.A., 2012. The Caspian Sea shelf during the Pleistocene regressive epochs. Oceanology 52 (4), 526-539.
Torres, M.A., 2007. The petroleum geology of western Turkmenistan: The Gograndag-Okarem province, in P.O. Yilmaz and G.H. Isaksen, (Eds.), Oil and gas of the Greater Caspian area: AAPG Studies in Geology 55, p. 109–132.
Tudryn, A., Chalié, F., Lavrushin, Yu.A., Antipov, M.P., Spiridonova, E.A., Lavrushin, V., Tucholka, P., Leroy, S.A.G., 2013. Late Quaternary Caspian Sea environment: Late Khazarian and Early Khvalynian transgressions from the lower reaches of the Volga river. Quaternary International 292, 193-204.
Tudryn, A., Leroy, S.A.G., Toucanne, S., Gibert-Brunet, E., Tucholka, P., Lavrushin, Y.A., Dufaure, O., Miska, S., Bayon, G., 2016. The Ponto-Caspian basin as a final trap for southeastern Scandinavian ice-sheet meltwater. Quaternary Science Reviews 148, 29-43.
Varushchenko, S., Varushchenko, A., Klige, R., 1987. Changes in the regime of the Caspian Sea and closed basins in time. Nauka, Moscow.
Yanina, T.A., 2013. Biostratigraphy of the Middle and Upper Pleistocene of the Caspian Region. Quaternary International 284, 85-97.

1003 Yanina, T.A., 2014. The Ponto-Caspian region: Environmental consequences
1004 of climate change during the Late Pleistocene. Quaternary International
1005 345, 88-99.
1006 Yanko-Hombach, V., 2007. Controversy over Noah's flood in the Black Sea:
1007 Geological and foraminiferal evidence from the shelf. In Yanko-Hombach,
1008 V., Gilbert, A.S., Panin, N. & Dolukhanov, P.M. (Eds.), The Black Sea
1009 Flood Question: Changes in Coastline, Climate, and Human Settlement.
1010 Springer, Dordrecht, 149–203.
1011 Wanner, H., Beer, J., Bütikofer, J., Crowley, T.J., Cubasch, U., Flückiger, J.,
1012 Goosse, H., Grosjean, M., Joos, F., Kaplan, J.O., Küttel, M., Müller, S.,
1013 Prentice, I.C., Solomina, O., Stocker, T.F., Tarasov, P., Wagner, M.,
1014 Widmann, M., 2008. Mid- to late Holocene climate change: an overview.
1015 Quaternary Science Reviews 27, 1791-1828.
1016 Zenina, M.A., Ivanova, E.V., Bradley, L.R., Murdmaa, I.O., Schornikov, E.I.,
1017 Marret, F., 2017. Origin, migration pathways, and paleoenvironmental
1018 significance of Holocene ostracod records from the northeastern Black
1019 Sea shelf. Quaternary Research 87, 49–65.

Supplementary Information

SI 1: Complete dinocyst record of core GS18

Fig. SI 1 Leroy et al.

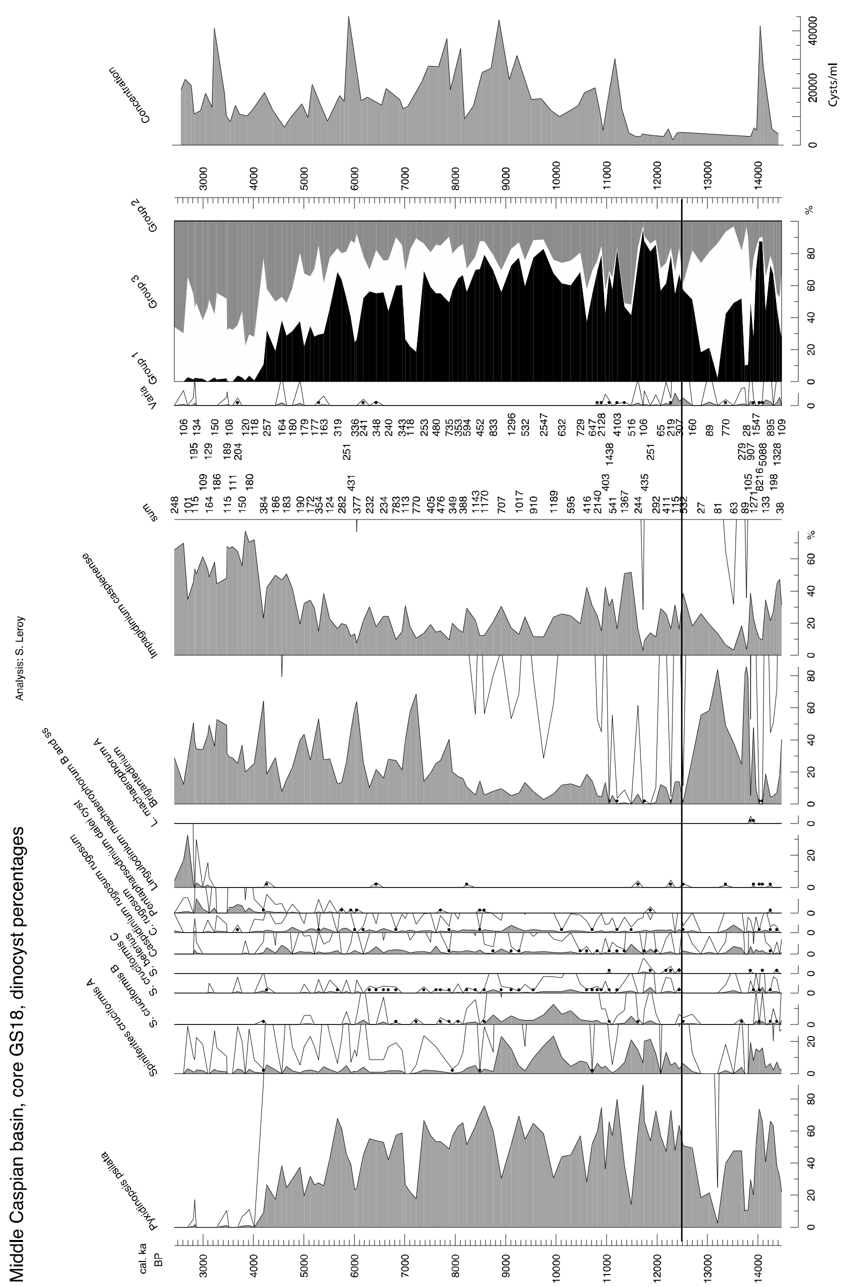

__Fig. SI 1__: Percentage dinocyst diagram of core GS18. The black line at 12.44 cal. ka BP separates the 22 new samples (bottom) from the published part (Leroy et al. 2014) (top). Black dots indicate percentages lower than 0.5%. ×10 exaggeration curves. Cumulative diagram to the right with groups as defined in Table 2.

SI 2: Radiocarbon dates of core Sh7

Table SI 2*: Radiocarbon dates of core Sh7. Dates obtained by G. Bayon and S. Toucanne (IFREMER).*

Sample name & depth in cm	Laboratory no	Age ^{14}C BP	Material
Core 7, 0-5	Poz-79790	4270 ± 70	ostracods
Core 7, 60-63	Poz-79792	2250 ± 60	ostracods
Core 7, 206-210	Poz-79793	8710 ± 60	ostracods
Core 7, 310-315	Poz-79794	7150 ± 70	ostracods
Core 7, 415-420	Poz-79795	2880 ± 70	ostracods
Core 7, 526	Beta 326989	13,270 ± 60	ostracods

SI 3: Palynological diagram and chronology of core Sh7

In addition to the commonly-used zonation on the upland pollen data (e.g. for changes in the terrestrial environment) and on the dinocyst data (e.g. for changes in the marine environment), a zonation based on changes in the total dispersion (CONISS), combining all palynomorphs (pollen, non-pollen palynomorphs and dinocysts) and including also total concentrations of pollen and dinocysts, has been made on the Sh7 sequence. This is in order to highlight major discontinuities in palynomorph diagrams and, therefore, taphonomy. This is essential to identify before any environmental interpretation.

The zonation on all palynomorphs has highlighted four main taphonomical changes at 422.5 (I), 145 (II), 514 (III) and 385 (IV) cm depth in order of decreasing importance (based on total dispersion of the cluster analysis, Fig. 3).

SI 3.1 Palynological diagram: results and interpretation

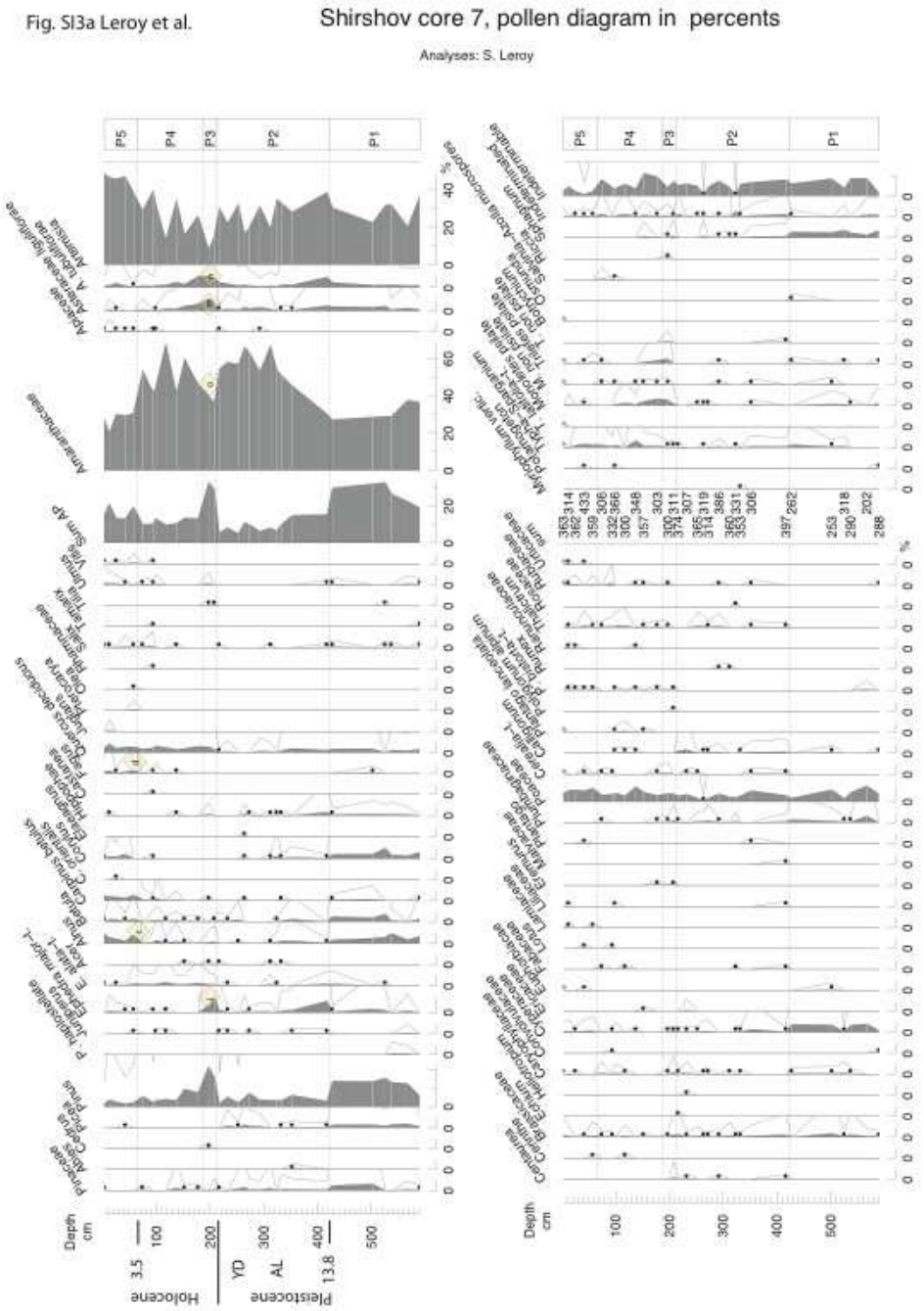

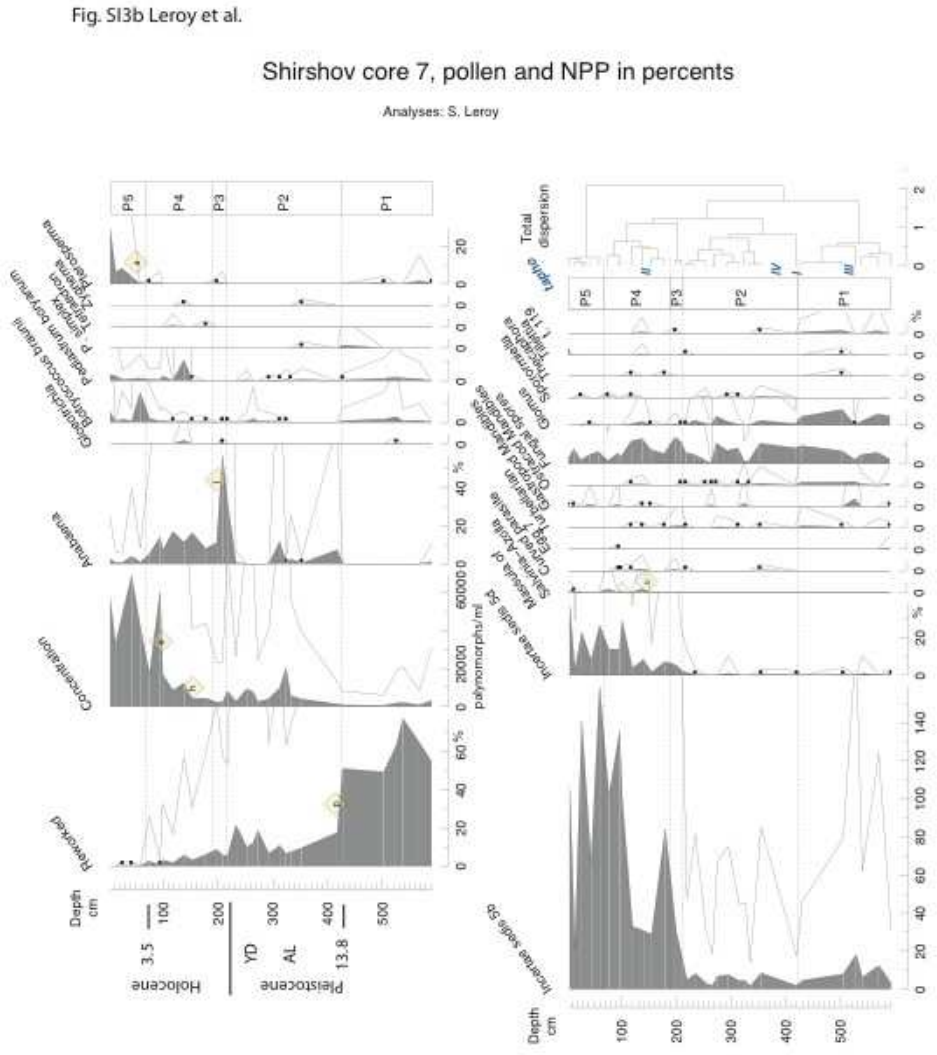

Figure SI 3: Palynological diagram of core Sh7. Black dots indicate percentages lower than 0.5%. Pollen, spores and non-pollen palynomorphs percentages are calculated on the sum of the upland pollen. Concentration of palynomorphs is shown in palynomorphs per ml of wet sediment. The zonation was performed by CONISS analysis after square-root transformation of upland pollen percentages. Al = Allerød. YD = Younger Dryas. Blue Roman numbers for the taphonomical change (tapho I to IV) in the total diagram. Letters in yellow lozenge are tie points (more information in Table SI 3).

The zonation performed on the pollen record of core Sh7 has allowed to identify five pollen zones (P1 to P5; Fig. SI 3). Zone P1 (590-422 cm) is characterised by large values of Pinaceae, *Picea, Pinus, Alnus, Betula* and *Corylus*, leading to the highest arboreal pollen (AP) percentages of the entire pollen record. However, the notable reworking percentages (up to 70%) suggest river transport and reworked material brought by river. This is most likely by the Volga River, as seen in core GS18 based on clay mineralogy and Nd isotopes (Tudryn et al. 2016). The large values of *Sphagnum* and *Glomus*

(indicator of soil erosion) together with the very low total pollen concentration (mostly <3000 palynomorphs ml^{-1}) support this interpretation. The zone P1/P2 boundary corresponds to the main of the four taphonomical changes in the total diagram (I).

In zone P2 (422-212 cm), the reworking drops below 20% (tie point p) and the AP values reach a minimum, consisting mainly of *Pinus* and *Ephedra,* with the last *Picea*. Amaranthaceae and *Artemisia* show increasing percentages across this zone until they dominate. The total pollen concentration increases, although it remains with low values (mostly <10,000 palynomorphs ml^{-1}). These results seem to indicate river influence on this site, although not as notoriously as in zone P1.

Zone P3 (212-187 cm) comprises two samples that stand out because of the increasing percentages of *Pinus*, *Ephedra* (tie point j) and Asteraceae liguliflorae and tubuliflorae (tie point m and n), the decreasing values of Amaranthaceae (tie point o) and *Artemisia*, and the occurrence of various fern spores. In addition, *Quercus* initiates a continuous curve. This zone begins with a very high peak of *Anabaena* (tie point l), probably linked to surface water warming at the beginning of the Holocene as seen in the pollen records of cores GS05 and GS18.

Pinus values progressively decrease across zone P4 (187-66 cm), while mesophilous tree taxa become more frequent. The percentages of Asteraceae decrease, while those of Amaranthaceae and *Artemisia* increase. *Salvinia-Azolla* appears at 137.5 cm (tie point i) and various algae reach high values. Reworked elements fade away, while total pollen concentration increases to reach high values (up to 60,000 palynomorphs ml^{-1}, tie points h and e). The taphonomical change at 145 cm (the second most important one) does not correspond to a main change in pollen zonation.

Zone P5 (66-2.5 cm) shows the expansion of some trees with the increasing values of *Alnus* (tie point c), *Betula, Carpinus betulus, Corylus, Fagus* (tie point d) and *Ulmus*. In addition, the values of Amaranthaceae drop, while *Artemisia* percentages attain a maximum. Total pollen concentration is maximal. *Botryoccocus* and *Pterosperma* peak (tie point a). This zone is the most different from the other zones.

SI 3.2 Chronology

Sixteen prominent tie points have been found when comparing core Sh7 with cores GS18 (above 666 cm depth, thus above any significant reworking; see reworked pollen curve in Tudryn et al. 2016) and GS05 (Table SI 3), combining common major changes, disappearances and appearances in pollen (twelve tie points) and dinocysts (four tie points), showing a chronological coherence (Fig. 2). A relative chronology may thus be suggested. It is immediately clear that none of the radiocarbon dates are valid (Table SI2).

***Table SI 3**: Chronological tie points for core Sh7 (middle basin) after the comparison of its palynological records with those from core GS18 (middle basin; [1] Leroy et al. 2014; [2] Tudryn et al. 2016) and core GS05 (south basin; [3] Leroy et al. 2013c).*

Line in Fig. 2	cm in Sh7	Observations in core Sh7 and core GS18	Age in cal. ka BP	Comparative sequence
a b	42	Start of *Pterosperma* Start of *L. machaerophorum*	2.7 3.2	GS18 [1] GS18 [1]
c d	57.5	Start continuous curve of *Alnus* Start continuous curve of *Fagus*	3.5 3.5	GS18 [1] GS18 [1]
e	94	Further step in pollen concentration increase	3.5	GS18 [1]
f	127.5	Zone d-4/d-5 boundary in GS18	4.1	GS18 [1]
g h i	137.5	Start of *P. dalei* Increase in pollen concentration First *Salvinia-Azolla*	6.0 8.2 9.2	GS18 [1] GS18 [1] GS18 [1]
j	197.5-208	High values of *Ephedra*	11.2- 11.1 11.5	GS18 [1] GS05 [3]
k l m-n	208	Peak of dinocyst concentration Peak of *Anabaena* Increase of Liguliflorae and Tubuliflorae	11.2 11.3 11.5	GS18 [1] GS18 [1] GS05 [3]
o	208	Low Amaranthaceae	10.8	GS18 [1]
p	427.5- 417.5	Drop in reworked pollen	13.8	GS18 [2]

SI 3.3 Comments on taphonomical changes

Taphonomical change I, at 422.5 cm, is the strongest one (highest total dispersion in Fig. 2): it corresponds to a sharp drop of reworked pollen and tie point p. It is close to a sharp change in lithology from non-oxidized to oxidized sediment It correlates to similar assemblage change in core GS18, at 13.8 cal. ka BP. This date has been shown elsewhere to correspond to when the Eurasian ice sheet had sufficiently retreated that its meltwater is not flowing directly anymore to the Volga drainage basin (Tudryn et al. 2016): shift from illite to smectite and drop of reworked palynomorphs.

Taphonomical change II, at 145 cm, is within one sample of the upper boundary of dinozone D4 (significant shift from *P. psilata* to *I. caspienense*) and corresponds to tie points f to i. This change is centred on the silty layer at 137.5 cm depth and is estimated at 4.1 cal. ka BP, when core GS18 (middle basin) and core CP14 (south basin) have the same major dinocyst turnover.

Taphonomical change III, at 514 cm, is one sample above dinozone D1/D2 boundary. Taphonomical change IV at 385 cm corresponds to the D2/D3 boundary.

One of the four main taphonomical changes (Fig. 2, 3 and SI3) correspond a pollen zone limit (I) and three to dinozone zone limits (II, III and IV). None of the taphonomical changes corresponds to both major pollen and dinocyst zone limits, underlining that the terrestrial and aquatic systems are

decoupled. In the light of the proposed chronology they probably correspond to sediment hiatus, with mass-wasting events at the origin.